

Video Article

Tangential Flow Ultrafiltration: A “Green” Method for the Size Selection and Concentration of Colloidal Silver Nanoparticles

Catherine B. Anders¹, Joshua D. Baker¹, Adam C. Stahler¹, Austin J. Williams¹, Jackie N. Sisco², John C. Trefry², Dawn P. Wooley², Ioana E. Pavel Sizemore¹

¹Department of Chemistry, Wright State University

²Department of Neuroscience, Cell Biology, and Physiology, Wright State University

Correspondence to: Dawn P. Wooley at dawn.wooley@wright.edu, Ioana E. Pavel Sizemore at ioana.pavel@wright.edu

URL: <https://www.jove.com/video/4167>

DOI: [doi:10.3791/4167](https://doi.org/10.3791/4167)

Keywords: Chemistry, Issue 68, Biomedical Engineering, Chemical Engineering, Nanotechnology, silver nanoparticles, size selection, concentration, tangential flow ultrafiltration

Date Published: 10/4/2012

Citation: Anders, C.B., Baker, J.D., Stahler, A.C., Williams, A.J., Sisco, J.N., Trefry, J.C., Wooley, D.P., Pavel Sizemore, I.E. Tangential Flow Ultrafiltration: A “Green” Method for the Size Selection and Concentration of Colloidal Silver Nanoparticles. *J. Vis. Exp.* (68), e4167, [doi:10.3791/4167](https://doi.org/10.3791/4167) (2012).

Abstract

Nowadays, AgNPs are extensively used in the manufacture of consumer products,¹ water disinfectants,² therapeutics,^{1,3} and biomedical devices⁴ due to their powerful antimicrobial properties.³⁻⁶ These nanoparticle applications are strongly influenced by the AgNP size and aggregation state. Many challenges exist in the controlled fabrication⁷ and size-based isolation^{4,8} of unfunctionalized, homogenous AgNPs that are free from chemically aggressive capping/stabilizing agents or organic solvents.⁷⁻¹³ Limitations emerge from the toxicity of reagents, high costs or reduced efficiency of the AgNP synthesis or isolation methods (e.g., centrifugation, size-dependent solubility, size-exclusion chromatography, etc.).^{10,14-18} To overcome this, we recently showed that TFU permits greater control over the size, concentration and aggregation state of Creighton AgNPs (300 ml of 15.3 $\mu\text{g ml}^{-1}$ down to 10 ml of 198.7 $\mu\text{g ml}^{-1}$) than conventional methods of isolation such as ultracentrifugation.¹⁹

TFU is a recirculation method commonly used for the weight-based isolation of proteins, viruses and cells.^{20,21} Briefly, the liquid sample is passed through a series of hollow fiber membranes with pore size ranging from 1,000 kD to 10 kD. Smaller suspended or dissolved constituents in the sample will pass through the porous barrier together with the solvent (filtrate), while the larger constituents are retained (retentate). TFU may be considered a “green” method as it neither damages the sample nor requires additional solvent to eliminate toxic excess reagents and byproducts. Furthermore, TFU may be applied to a large variety of nanoparticles as both hydrophobic and hydrophilic filters are available.

The two main objectives of this study were: 1) to illustrate the experimental aspects of the TFU approach through an invited video experience and 2) to demonstrate the feasibility of the TFU method for larger volumes of colloidal nanoparticles and smaller volumes of retentate. First, unfunctionalized AgNPs (4 L, 15.2 $\mu\text{g ml}^{-1}$) were synthesized using the well-established Creighton method^{22,23} by the reduction of AgNO_3 with NaBH_4 . AgNP polydispersity was then minimized via a 3-step TFU using a 50-nm filter (460 cm^2) to remove AgNPs and AgNP-aggregates larger than 50 nm, followed by two 100-kD (200 cm^2 and 20 cm^2) filters to concentrate the AgNPs. Representative samples were characterized using transmission electron microscopy, UV-Vis absorption spectrophotometry, Raman spectroscopy, and inductively coupled plasma optical emission spectroscopy. The final retentate consisted of highly concentrated (4 ml, 8,539.9 $\mu\text{g ml}^{-1}$) yet lowly aggregated and homogeneous AgNPs of 1-20 nm in diameter. This corresponds to a silver concentration yield of about 62%.

Video Link

The video component of this article can be found at <https://www.jove.com/video/4167/>

Protocol

1. Synthesis of Colloidal AgNPs

The reaction mechanism for the Creighton method (slightly modified, inexpensive)²² is described in great detail in the Supporting information of reference Pavel et.al together with the undesired hydrolysis side-reaction of NaBH_4 at room temperature or higher.²³

1. Clean all glassware for 12-24 hr in a 10% HNO_3 bath, then for 4-12 hr in a 1.25 M NaOH in 40% ethanol bath, and finally autoclave. Glassware should be rinsed thoroughly a minimum of five times with ultrapure water (17 M Ω or higher) after the acid and base bath steps.
2. Prepare 300 ml of a 2 mM NaBH_4 solution and 100 ml of a 1 mM AgNO_3 solution using autoclaved water cooled at 10 °C. The lower temperatures will prevent the side-reaction of NaBH_4 .
3. Add 300 ml of 2 mM NaBH_4 solution to a 500 ml Erlenmeyer reaction flask containing a stir bar and wrap the flask with aluminum foil to prevent silver oxidation. Place the flask in an ice bath on a stir plate and stir the solution at 325 rpm for 10 min.

4. Prime a 25 ml burette by rinsing with a full column of ultrapure water. After priming, fill the burette with AgNO₃ solution and wrap with aluminum foil.
5. In a dark room, add 50 ml of 1 mM AgNO₃ solution at a rate of 1 drop sec⁻¹ to the NaBH₄ solution with continuous stirring (**Figure 1A**). Cover the middle section of the apparatus with a "foil tent" to minimize light exposure during the AgNO₃ addition. The AgNO₃ addition will require 30-40 min. Replenish the ice bath periodically.
6. After the AgNO₃ addition is complete, replenish the ice bath and continue stirring the colloidal solution for an additional 45-50 min. The formation of colloidal AgNPs is signaled by a change in color from colorless to a golden yellow, which is characteristic of the surface plasmon resonance maximum of AgNPs (**Figure 1B**).
7. Once the reaction is completed, refrigerate the colloid. Colloidal AgNP batches may be combined after one week if the colloid has remained consistent, *i.e.*, the colloidal solution has not aggregated and the batch has been characterized using UV-Vis absorption spectrophotometry and Raman spectroscopy to identify possible aggregation or contaminants.

2. Characterization of Colloidal AgNPs

A Cary 50 UV-VIS-NIR spectrophotometer (Varian Inc.) and a LabRamHR 800 Raman system (Horiba Jobin Yvon, Inc.) equipped an Olympus BX41 confocal Raman microscope, were utilized for AgNP characterization. The Cary WinUV software, LabSpec v.5 and Origin 8.0 software were employed for the data collection and analysis.

Note: The acquisition parameters will have to be optimized for other instrumentation models.

Determination of Surface Plasmon Resonance of Colloidal AgNPs via UV-Vis Spectrophotometry

1. Fill a 1 cm³ disposable cuvette with Creighton colloid and ultrapure water in a 1:10 volume ratio. Fill another 1 cm³ cuvette with ultrapure water for a blank baseline correction. Wipe the outside of both cuvettes with a Kimwipe.
2. Set the spectrophotometer to absorbance mode from a Y minimum of -0.5 to a Y maximum of 1.0. Set the X scanning window to 200-800 nm and select a fast scan rate of 4,800 nm min⁻¹ with baseline correction.
3. Insert the cuvette filled with water into the instrument and run a baseline scan. Repeat if necessary until a non-zero baseline control is achieved.
4. Replace the blank cuvette with the sample cuvette and initiate an absorbance scan for the collection of the UV-Vis absorption spectrum of the colloidal sample (**Figure 1C**).

Purity Test of Colloidal AgNPs via Raman spectroscopy

Due to the time limitation of the video demonstration (10-15 min video) and the space limitation of the protocol text (maximum 3 pages), this experimental section will not be videotaped.

5. Set the instrument parameter settings as follows: excitation source (632.8 nm He-Ne), filter (no filter, laser power at the sample ~ 17 mW), confocal hole (300 μm), spectrometer (730 cm⁻¹), holographic grating (600 grooves/mm), objective lens (50x long working distance air objective), exposure time (30 s), and accumulation cycles (5).
6. Use a clean pipette to fill a 2 ml quartz cuvette with colloid and gently insert the plug. Use a Kimwipe to clean off fingerprints, smudges or colloid from the surface of the cuvette. Significantly lower the microscope stage. Select the 50x objective lens and place the cuvette onto the stage.
7. Focus the laser beam on the AgNP colloid directly underneath the inner wall of the cuvette using the video mode of the instrument and the Olympus camera. Turn off room lights and acquire Raman spectrum (**Figure 1D**).

3. Size-selection and Concentration of Colloidal AgNPs via Tangential Flow Ultrafiltration (TFU)

A KrosFlo II Research filtering system (Spectrum Laboratories, Rancho Dominguez, CA) was used to limit the AgNP polydispersity and to concentrate them (**Figure 2**). The three steps of the TFU process were: (1) Size-selection of AgNPs and AgNP-aggregates of 50-nm in diameter and larger using a 50-nm MidiKros polysulfone module (460 cm²), (2) Size selection and concentration of AgNPs of 1-20 nm in diameter using a 100-kD MidiKros filter (200 cm²), and (3) Further volume reduction using a 100-kD MicroKros polysulfone filter (20 cm²) (**Figure 3**).

Step 1

1. Connect the size 17 MasterFlex feeding tubing to the peristaltic pump according to **Figure 2A**. A Y-junction and a tubing junction will be needed for the set-up. Attach tubing to the 50-nm MidiKros module. Be sure to secure tubing to filter using zip ties. Select tubing size 17 using SIZE button.
2. Select counterclockwise pump direction using DIR button. Make sure MODE button is on INT.
3. Lower the pump rate to below 300 ml min⁻¹ before starting pump. The pump rate should be adjusted according to the size of the used tubing. It should be a small setting to permit the operator to promptly react to potential leaks but large enough to still have an effect of priming the system. In order to create the vacuum needed to draw colloid from the reservoir into the tubing and filter, cut the tubing that leads from the bottom section of the filter to the top portion of the Y-junction in the middle of the tubing.
4. Place the section of tubing that leads from the filter into the reservoir bottle and clamp off the bottom section of tubing near the Y-junction with a clamp or by hand. Turn on the pump. The created vacuum should begin siphoning the colloid.
5. Once the liquid is flowing freely through the tube, turn off the pump, join the broken section of tubing with a tubing junction and secure with zip ties. Turn on the pump again and continue filtration.

6. Check the tubing circuit for leaks. If a leak is found, fix the leak by adjusting the fitting or re-securing with a zip tie. Once the tubing system is leak free, the pump flow rate may be increased to no greater than 700 ml min^{-1} . This pump rate value should be optimized according to tubing size to avoid tubing failure. Continue filtration until the liquid in the reservoir bottle is depleted to nearly nothing.
7. Once the filtration is complete, collect the filtrate that contains AgNPs of 50-nm diameter and smaller. The retentate may be saved for further analysis according to the specific AgNP application.

Step 2

8. Rinse the tubing with 2% HNO_3 and ultrapure water prior to installing the 100-kD MidiKros filter using the same setup as for the 50-nm module.
9. Repeat step 3.3 using the 100-kD MidiKros module.
10. Once the filtration is complete, collect the contents of the tubing and the filter (100-kD retentate). The volume should be approximately 50 ml.

Step 3

11. Connect the size 14 MasterFlex tubing and the 100-kD MicroKros FILTER to the peristaltic pump according to **Figure 2B**. Secure all junctions with zip ties. Select tubing size 14 on the pump using the SIZE button and lower the pump rate to 30 ml min^{-1} .
12. Begin the filtration process. Check the tubing circuit for leaks. If a leak is found, fix the leak by adjusting the fitting or re-securing with a zip tie.
13. Once the tubing system is leak free, the pump flow rate may be increased to no greater than 90 ml min^{-1} . Continue filtration until the liquid remaining in the reservoir bottle contains a minimal amount of concentrate.
14. The remaining contents of the tubing and filter can be collected into the reservoir bottle by removing the feeding tube from the bottle while the pump is still running. Once the tubing and filter contents are in the reservoir bottle, the pump may be turned off.

4. Quantification of Silver Amount in Colloidal AgNPs by Inductively Coupled Plasma Optical Emission Spectroscopy (ICP-OES)

Each colloidal sample was chemically digested and the amount of silver was quantified by ICP-OES using an A 710E spectrometer (Varian Inc.). A linear regression calibration curve for silver (**Figure 4**) was constructed using eight silver standards ($0, 3, 7, 10, 15, 25, 50$, and $100 \mu\text{g L}^{-1}$), which were prepared from a $10,000 \mu\text{g ml}^{-1}$ silver standard for trace metal analysis (Ultra Scientific).

1. Chemically digest samples using HNO_3 . The representative samples are the original colloid (step 1), 50-nm filtrate (step 1), 100-kD retentate (step 2), and final 100-kD retentate (step 3) (**Figure 3**).
2. The samples should be diluted with 2% HNO_3 using the following volume ratios: 1:1000 for the original colloid, 1:1000 for the 50-nm filtrate, 1:25,000 for the first 100-kD retentate, and 1:250,000 for the final 100-kD retentate. To prevent silver leaching, all samples should be stored in low-density polypropylene containers.
3. Set the ICP-OES instrument parameters as follows: wavelength for Ag (328.068 nm), power (1.20 kW), plasma flow (15.0 L min^{-1}), auxiliary flow (1.50 L min^{-1}), and nebulizer pressure (200 kPa).
4. Each sample should be measured in triplicate with a replicate time of 10 s. Between-measurement stabilization time of 15 sec and a 30 sec sample uptake delay should be used. A method blank should be introduced between every sample to reduce potential cross-contamination.

5. Size Distribution of Colloidal AgNPs via Transmission Electron Microscopy (TEM)

A Phillips EM 208S TEM was used to visualize the colloidal AgNPs. Electron micrographs were captured using a high resolution Gatan Bioscan camera and analyzed in ImageJ software.²⁴

1. Dilute the 100-kD retentate sample with ultrapure water (1:100 volume ratio). Deposit $20 \mu\text{l}$ of the original colloid and the diluted 100-kD retentate (step 3) on 300-mesh formvar-coated gold grids (Electron Microscopy Sciences). Allow the grids to dry in a desiccator. View within one day.
2. Set the accelerating potential of the TEM instrument at 70 kV to visualize AgNPs. Capture electron micrographs (**Figure 5**) using the high-resolution camera and save as tagged image files format (tiff).

6. Representative Results

Synthesis and Characterization of Colloidal AgNPs

Four liters of Creighton colloidal AgNPs were successfully synthesized using the setup displayed in **Figure 1A**. The final colloid had a characteristic golden yellow color (**Figure 1B**).^{22, 23} The UV-Vis absorption spectrum of this colloid had a typical sharp, symmetrical surface plasmon peak (SPR) at 394 nm (**Figure 1C**). The Raman spectrum of the original Creighton colloid and the final 100-kD retentate presented only three vibrational modes, namely the bending (1640 cm^{-1}) and symmetric and asymmetric stretching modes of H_2O (3245 cm^{-1} and 3390 cm^{-1} , respectively) (**Figure 1D**).

TFU of Colloidal AgNPs

The TFU setup and the schematic of the 3-step TFU process are depicted in **Figures 2 and 3**, respectively. In step 1, a 50-nm filter (460 cm^2) was utilized to size-select and to remove AgNPs and AgNP-aggregates of 50-nm diameter and larger from the original colloid (about 100 ml of 50-nm retentate). This step was also accompanied by a small volume reduction from 4 L of original colloid down to 3.9 L of 50-nm filtrate. No backwashing or flow disruption step was used. The largest volume reduction (*i.e.*, water removal) was obtained in step 2, when the 50-nm filtrate was subsequently run through a 100-kD filter (200 cm^2). The resulting 100-kD retentate had a total volume of 50 ml. Most of the synthesis byproducts and excess reagents were eliminated in this step through the water solvent (3.850 ml of 100-kD filtrate). Further, AgNP concentration

was achieved by the addition of a third filtration step to the previously reported procedure.¹⁹ In this step 3, a 100-kD filter of a smaller surface area (20 cm²) reduced the 100-kD retentate volume to 4.0 ml. The TEM measurements will demonstrate that this final 100-kD retentate consists mostly of lowly aggregated AgNPs of 1-20 nm in diameter.

ICP-OES and TEM of Colloidal AgNPs

A linear regression calibration curve (**Figure 4**) for silver was constructed from eight standards (0, 3, 7, 10, 15, 25, 50, and 100 µg L⁻¹). The amount of silver in each of the four representative colloidal samples was then determined from the ICP-OES calibration curve through extrapolation: original colloid (15.2 ppm, **Figure 3A**), 50-nm filtrate (14.1 ppm, **Figure 3B**), first 100-kD retentate (683.1 ppm, **Figure 3C**) and final 100-kD retentate (8,538.9 ppm, **Figure 3D**). The actual yield of 15.2 ppm is very close to the typical theoretical yield of 15.4 ppm for the Creighton reaction. The extreme concentration of AgNPs (4 ml of 8,538.9 ppm) was reflected by a dramatic change in color from golden yellow for the original colloid to dark brown for the final 100-kD retentate (**Figure 3**, insets of vial pictures). The quality of the filters was found to be critical to the TFU process, in particular to step 1. The final retentate concentrations ranged from 3,390.1 ppm to 9,333.3 ppm depending on the condition of the filters (heavily used versus brand new). If the membrane pores become compromised, AgNPs that have diameters less than 50-nm will also be retained and will subsequently decrease the overall amount of AgNPs that is collected in the filtrate. Optimization of the filtration process to include pressure monitoring and proper cleaning can increase the life span of the filters.

Representative TEM micrographs of the original Creighton colloid and the final 100-kD retentate (step 3) are shown in **Figure 5A and 5C**, respectively. In their unaggregated state, AgNPs appear as black round areas on a lighter grey background. Approximately 800 AgNPs were identified in the TEM micrographs of each of the two samples and were analyzed using the Image J software. One particle was defined by a complete and enclosed perimeter. An area threshold value was set at 1.0 nm² according to the resolution of the TEM micrographs. The AgNP counts and area data were then exported into Microsoft Excel and the AgNP diameters were extrapolated. The average AgNP diameter in the original colloid and the final 100-kD retentate were determined to be 9.3 nm and 11.1 nm, respectively. The diameter measurements of the AgNPs were then exported to Origin 8.0 software and a TEM size histogram was constructed for each sample (**Figure 5B and 5D**).

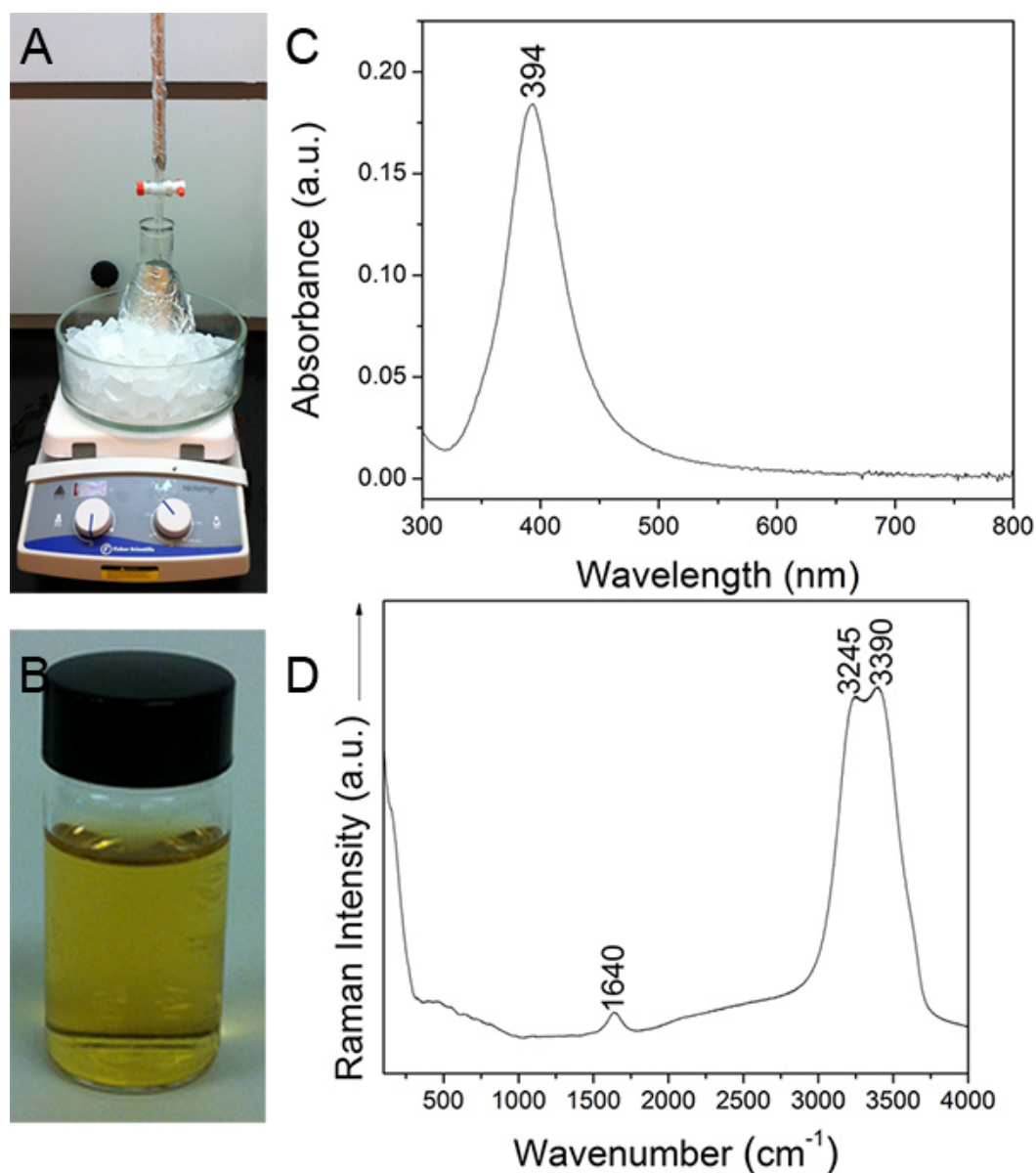


Figure 1. A) Synthesis setup, B) Characteristic color, C) UV-Vis absorption spectrum, and D) Raman spectrum of Creighton colloidal AgNPs.

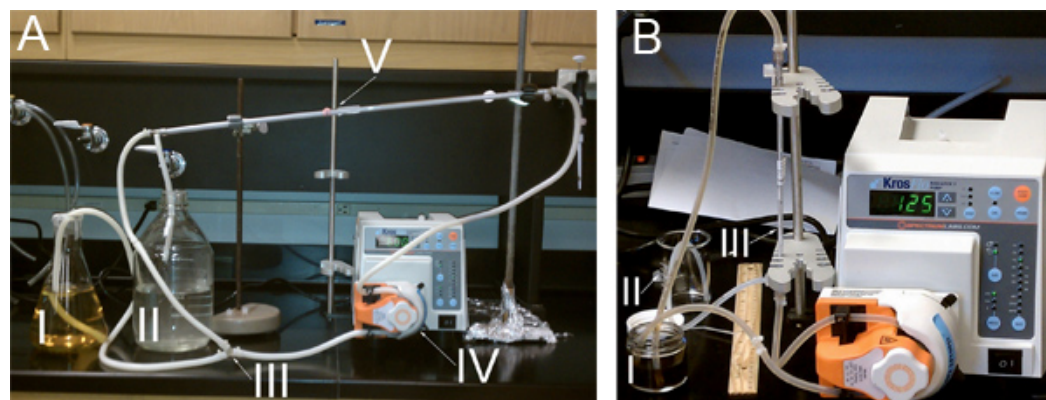


Figure 2. TFU experimental setup for **A)** steps 1 and 2: I) Reservoir containing Creighton colloidal AgNPs. II) Reservoir for filtrate collection. III) Y-junction in tubing. IV) Peristaltic pump head. V) Either 50-nm or 100-kD Midi Kros filter. **B)** step 3: I) Reservoir containing Creighton colloidal AgNPs. II) Reservoir for filtrate collection. III) 100-kD Micro Kros filter.

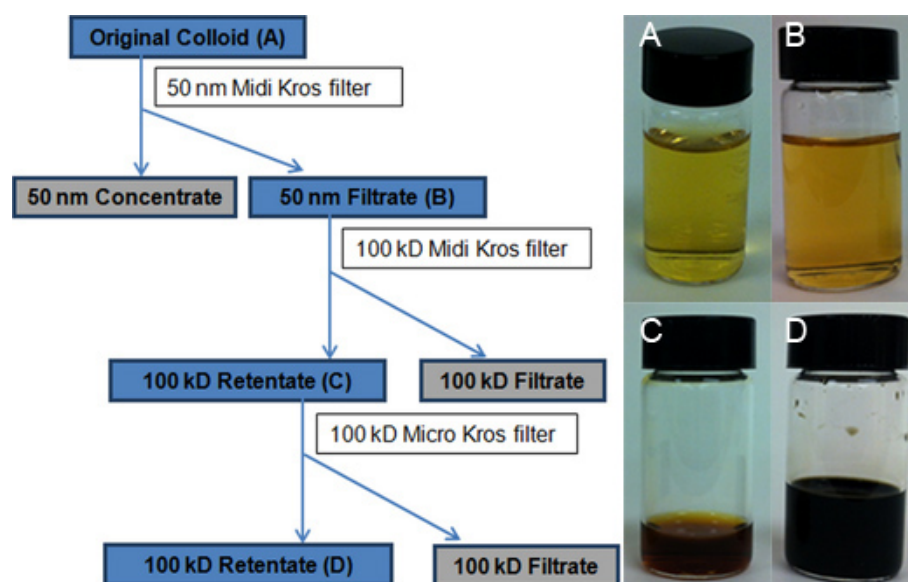


Figure 3. Flowchart depicting the TFU process. The blue-shaded boxes mark the colloidal suspensions of AgNPs collected for further analysis. Vial photographs show **A)** Original colloid batch, **B)** 50-nm filtrate collected after processing the original colloid through the 50-nm filter (460 cm²), **C)** first 100-kD retentate obtained after volume reduction using the 100-kD Midi Kros filter (200 cm²), and **D)** final 100-kD retentate resulting from the volume reduction using the 100-kD Micro Kros filter (20 cm²). The 100-kD filtrate looks like water.

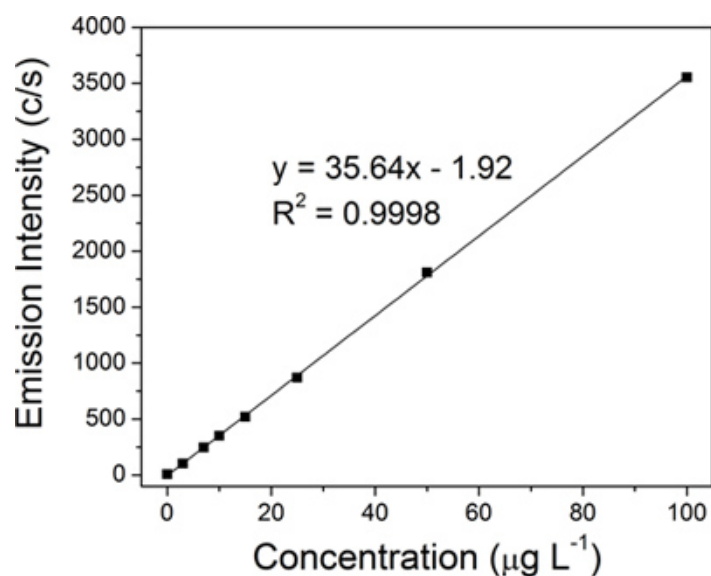


Figure 4. ICP-OES linear calibration constructed using eight silver standards: 0, 3, 7, 10, 15, 25, 50, and 100 µg L⁻¹.

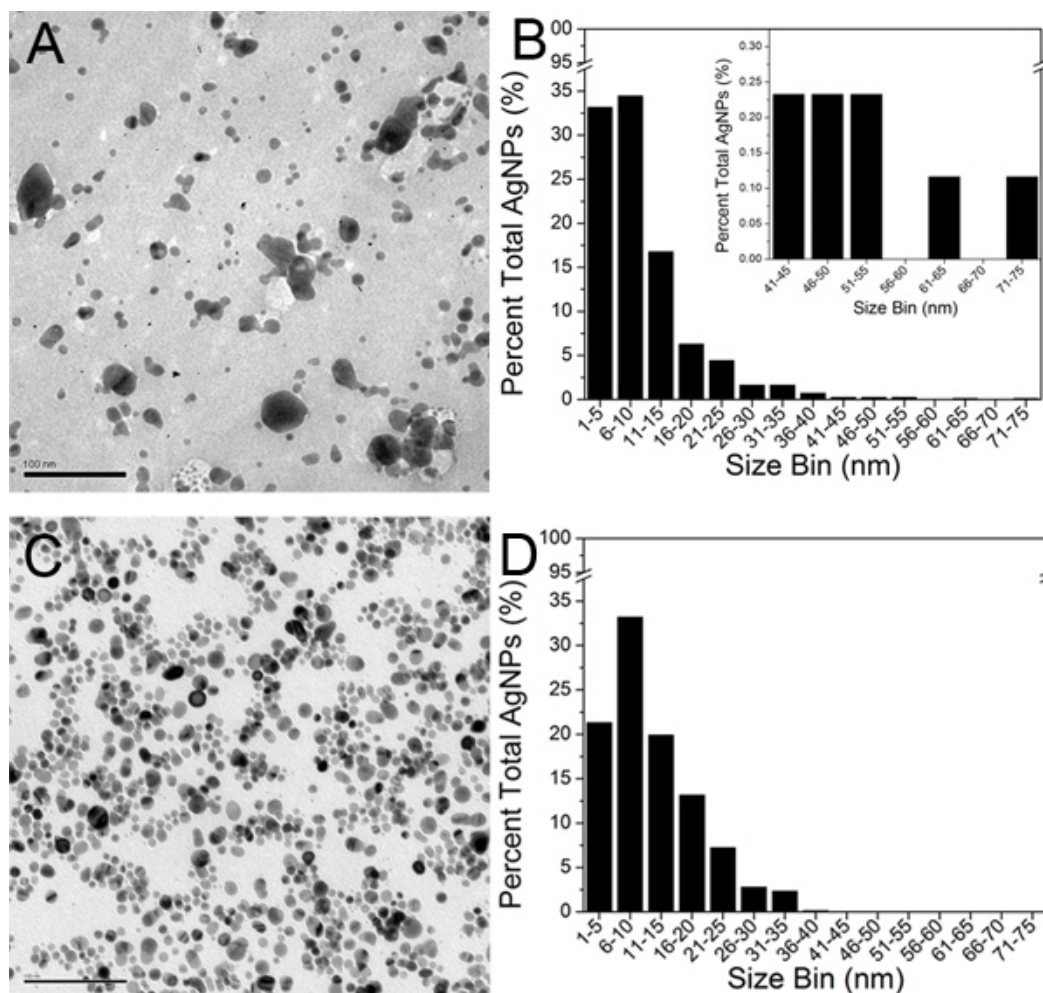


Figure 5. TEM micrographs of **A)** original Creighton AgNPs and **C)** final 100-kD retentate (scale bar is 100 nm). TEM size histograms constructed by analyzing approximately 800 AgNPs for **B)** original Creighton AgNPs, and **D)** final 100-kD retentate. The inset in **Figure 5B** shows the expanded 41-75 nm size range for comparison purposes. [Click here to view larger figure.](#)

Discussion

UV-Vis Absorption Spectrophotometry and Raman Spectroscopy of Colloidal AgNPs

It is well known that the number of surface plasmon resonance peaks in the absorption spectrum of a colloid decreases as the symmetry of the AgNPs increases. Additionally, AgNP aggregation leads to the appearance of broader or red-shifted peaks.^{25,26} The presence of a single, sharp and symmetrical SPR peak at 394 nm is indicative of small, spherical AgNPs of moderate aggregation and size distribution.

The purity of the colloidal samples before and after ultrafiltration was demonstrated by the Raman spectra of the original Creighton colloid and the final 100-kD retentate, which exhibited only three vibrational modes characteristic to H₂O. The Raman signal associated with organic impurities or ultrafiltration contaminants of large Raman cross-sections would be enhanced through the immediate proximity to the AgNP surface (i.e., the so-called surface-enhanced Raman spectroscopy (SERS) effect).

ICP-OES and TEM of Ultrafiltered Colloidal AgNPs

The addition of a third, 100-kD filtration step to the previously reported TFU procedure¹⁹ facilitated the successful reduction of a larger volume of Creighton colloidal AgNPs (4L batch of 15.2 ppm) in a 1,000-fold smaller volume of retentate (4 ml of 8,538.9 ppm). This corresponds to a TFU concentration yield of approximately 62% taking into account the amount of AgNPs and AgNP-aggregates of 50-nm diameter and larger that were removed. The degree of concentration is remarkable because the final 100-kD retentate mostly consisted of monodisperse AgNPs that were 1-20 nm in diameter and free from excess reagents and byproducts. The third, 100-kD filtration step improved the concentration yield from 45%²⁰ to 62%. Further TFU improvements in the size-selection and concentration of AgNPs could be obtained by utilizing additional hollow fiber membranes. Filters of pore size ranging from 1,000 kD to 10 kD and surface areas from 5.1 m² to 8 cm² are currently available for both hydrophobic and hydrophilic samples. Buffer exchange can also be performed during TFU, depending on downstream applications. When the volume reduction exceeds 800-fold (i.e., when the volume is reduced from 4 L to less than 5 ml), there is a decrease in the stability and shelf life of the colloidal suspension due to the extreme degree of concentration. The shelf life for these highly concentrated, unfunctionalized AgNP is approximately one to two weeks at 10 °C. While inconvenient, this limitation is managed through careful research planning and preparation. This

extreme degree of concentration was desired for ongoing nanotoxicity studies at various concentrations. Less concentrated batches of AgNPs are expected to have better stability and longer shelf life.

Visual inspection of the TEM images (**Figure 5A and 5C**) showed an increased frequency of minimally aggregated AgNPs in the final 100-kD retentate as compared with the original colloid. The TEM size histograms of the two colloidal samples (**Figure 5B and 5D**) further confirmed that the polydispersity of the Creighton colloidal AgNPs was limited through TFU. Further polydispersity limitation may be achieved by employing a series of filtration membranes of smaller pore sizes. The diameters of the Creighton AgNPs ranged from 1 nm to 75 nm (**Figure 5B** and the inset showing the expanded 41-75 nm size bins), while the AgNPs and/or AgNP-aggregates of 50 nm and larger (0.9% out of percent total AgNPs) were absent in the TEM size histogram of the final 100-kD sample (**Figure 5D**). The 100-kD retentate was comprised mostly of AgNPs that had diameters of 1-20 nm; there was a small contribution (12.4%) from AgNPs in the 21-40 size bins. **Figure 5B and 5D** confirmed that the size distribution trend was retained for the 100-kD retentate during the TFU process with the exception of the 1-5 nm size range. There was a noticeable decrease in the frequency of the smaller AgNPs of 1-5 nm in diameter for the 100-kD sample (from 33.2% to 21.3%), which was attributed to AgNP passage through the membrane filter into the filtrate. As a result, the average AgNP diameter increased from 9.3 nm for the original colloid to 11.1 nm for the final 100-kD retentate. Because approximately 800 AgNPs were analyzed for both colloidal samples, the decreased frequency of smaller AgNPs in the 1-5 nm (11.9%) and 6-10 nm (1.3%) size ranges was accompanied by a corresponding increase in the frequency of larger AgNPs in the 11-25 nm size bins (*i.e.*, about 12.8% from the original colloid to the 100-kD retentate).

In conclusion, TFU proved to be an efficient, "green" method for the size-selection and concentration of colloidal AgNPs with minimal aggregation at various volume scales. Eliminating the use of chemically aggressive reagents or organic solvents from the AgNP synthesis (for better size, shape, and aggregation control) may significantly reduce AgNP toxicity while improving their therapeutic index. AgNPs of limited polydispersity may find other immediate industrial and research applications due to their improved catalytic,²⁷ optoelectronic^{28, 29} or SERS-based biosensing properties.^{9, 19, 30, 31, 31} A very recent study by Lander *et al.*³² showed that micro and ultrafiltration membranes made of five different polymeric materials (polysulfone, polyethersulfone, nylon, cellulose acetate, and polyvinylidene fluoride) may be successfully implemented for the size selection of functionalized NPs. These NPs of 2-10 nm in diameter had Ag, Au or TiO₂ cores and were functionalized with organic polymer coatings that led to positive or negative surface charges. Both the cores and the surface functionality of the NPs were found to play a major role in the NP retention or passage through the membranes (0.2 nm to 0.22 μ m). As expected, the positively charged NPs were entirely rejected (> 99%) by the negatively charged membranes that had 20-times larger pore size than the NP diameters. From these experiments, one learns that the interaction mechanism should be carefully considered in future studies with functionalized NPs.

Disclosures

No conflicts of interest declared.

Acknowledgements

Funding from the National Science Foundation through the NUE in Engineering and the LEADER Consortium Programs is gratefully acknowledged.

References

1. The Project on Emerging Nanotechnologies. http://www.nanotechproject.org/inventories/consumer/analysis_draft/, (2011).
2. Savage, N. & Diallo, M.S. Nanomaterials and Water Purification: Opportunities and Challenges. *Journal of Nanoparticle Research*. **7**, 331-342 (2005).
3. Jain, J., *et al.* Silver Nanoparticles in Therapeutics: Development of an Antimicrobial Gel Formulation for Topical Use. *Mol. Pharmaceutics*. **6**, 1388-1401 (2009).
4. Dal Lago, V., Franca, d.O., de, A.G., Kobarg, J., & Borba Cardoso, M. Size-selective silver nanoparticles: future of biomedical devices with enhanced bactericidal properties. *J. Mater. Chem.* **21**, 12267-12273 (2011).
5. Panacek, A., *et al.* Silver Colloid Nanoparticles: Synthesis, Characterization, and Their Antibacterial Activity. *J. Phys. Chem. B*. **110**, 16248-16253 (2006).
6. Elechiguerra, J., *et al.* Interaction of silver nanoparticles with HIV-1. *Journal of Nanobiotechnology*. **3**, 6 (2005).
7. Jana, N.R., Sau, T.K., & Pal, T. Growing Small Silver Particle as Redox Catalyst. *J. Phys. Chem. B*. **103**, 115-121 (1999).
8. Tolaymat, T.M., *et al.* An evidence-based environmental perspective of manufactured silver nanoparticle in syntheses and applications: A systematic review and critical appraisal of peer-reviewed scientific papers. *Sci. Total Environ.* **408**, 999-1006 (2010).
9. Willets, K. Surface-enhanced Raman scattering (SERS) for probing internal cellular structure and dynamics. *Analytical and Bioanalytical Chemistry*. **394**, 85-94 (2009).
10. Novak, J.P., Nickerson, C., Franzen, S., & Feldheim, D.L. Purification of Molecularly Bridged Metal Nanoparticle Arrays by Centrifugation and Size Exclusion Chromatography. *Anal. Chem.* **73**, 5758-5761 (2001).
11. Hossain, M.K., Kitahama, Y., Huang, G.G., Han, X., & Ozaki, Y. Surface-enhanced Raman scattering: realization of localized surface plasmon resonance using unique substrates and methods. *Analytical and Bioanalytical Chemistry*. **394**, 1747-1760 (2009).
12. Henglein, A. & Giersig, M. Formation of Colloidal Silver Nanoparticles: Capping Action of Citrate. *J. Phys. Chem. B*. **103**, 9533-9539 (1999).
13. Sapsford, K.E., Tyner, K.M., Dair, B.J., Deschamps, J.R., & Medintz, I.L. Analyzing Nanomaterial Bioconjugates: A Review of Current and Emerging Purification and Characterization Techniques. *Anal. Chem.* **83**, 4453-4488 (2011).
14. Al-Somali, A., Krueger, K. M., Falkner, J.C., & Colvin, V.L. Recycling Size Exclusion Chromatography for the Analysis and Separation of Nanocrystalline Gold. *Anal. Chem.* **76**, 5903-5910 (2004).
15. Hanauer, M., Pierrat, S., Zins, I., Lotz, A., & Sonnichsen, C. Separation of Nanoparticles by Gel Electrophoresis According to Size and Shape. *Nano Lett.* **7**, 2881-2885 (2007).

16. Sweeney, S.F., Woehrle, G.H., & Hutchison, J.E. Rapid Purification and Size Separation of Gold Nanoparticles via Diafiltration. *J. Am. Chem. Soc.* **128**, 3190-3197 (2006).
17. Clarke, N.Z., Waters, C., Johnson, K.A., Satherley, J., & Schiffrin, D.J. Size-Dependent Solubility of Thiol-Derivatized Gold Nanoparticles in Supercritical Ethane. *Langmuir*. **17**, 6048-6050 (2001).
18. Schaaff, T.G., *et al.* Isolation of Smaller Nanocrystal Au Molecules: Robust Quantum Effects in Optical Spectra. *J Phys Chem B*. **101**, 7885-7891 (1997).
19. Trefry, J.C., *et al.* Size Selection and Concentration of Silver Nanoparticles by Tangential Flow Ultrafiltration for SERS-Based Biosensors. *J. Am. Chem. Soc.* **132**, 10970-10972 (2010).
20. Bhattacharjee, S., Bhattacharjee, C., & Datta, S. Studies on the fractionation of β and α -lactoglobulin from casein whey using ultrafiltration and ion-exchange membrane chromatography. *J. Membr. Sci.* **275**, 141-150 (2006).
21. Eppler, A., Weigandt, M., Schulze, S., Hanefeld, A., & Bunjes, H. Comparison of different protein concentration techniques within preformulation development. *Int. J. Pharm.* **421**, 120-129 (2011).
22. Creighton, J.A., Blatchford, C.G., & Albrecht, M.G. Plasma resonance enhancement of Raman scattering by pyridine adsorbed on silver or gold sol particles of size comparable to the excitation wavelength. *J. Chem. Soc. Faraday Trans. 2*. **75**, 790-798 (1979).
23. Pavel, I.E., *et al.* Estimating the Analytical and Surface Enhancement Factors in Surface-Enhanced Raman Scattering (SERS): A Novel Physical Chemistry and Nanotechnology Laboratory Experiment. *J. Chem. Educ.*, (2011).
24. Rasband, W.S. & ImageJ, U.S. National Institutes of Health, Bethesda, Maryland, USA, <http://imagej.nih.gov/ij/>, 1997-2011, (2011).
25. Kelly, K.L., Coronado, E., Zhao, L.L., & Schatz, G.C. The Optical Properties of Metal Nanoparticles: The Influence of Size, Shape, and Dielectric Environment. *J. Phys. Chem. B*. **107**, 668-677 (2003).
26. Šileikaitė, A., Prosyčevs, I., Puišo, J., Juraitis, A., & Guobienė, A. Analysis of Silver Nanoparticles Produced by Chemical Reduction of Silver Salt Solution. *Mater. Sci. (Medžiagotyra)*. **12**, 287-291 (2006).
27. Lewis, L.N. Chemical catalysis by colloids and clusters. *Chem. Rev.* **93**, 2693-2730 (1993).
28. Li, Y., Wu, Y., & Ong, B.S. Facile Synthesis of Silver Nanoparticles Useful for Fabrication of High-Conductivity Elements for Printed Electronics. *J. Am. Chem. Soc.* **127**, 3266-3267 (2005).
29. Sun, Y. & Xia, Y. Shape-Controlled Synthesis of Gold and Silver Nanoparticles. *Science*. **298**, 2176-2179 (2002).
30. Han, X., Zhao, B., & Ozaki, Y. Surface-enhanced Raman scattering for protein detection. *Analytical and Bioanalytical Chemistry*. **394**, 1719-1727 (2009).
31. Pavel, I., *et al.* Label-Free SERS Detection of Small Proteins Modified to Act as Bifunctional Linkers. *J. Phys. Chem. C*. **112**, 4880-4883 (2008).
32. Ladner, D.A., Steele, M., Weir, A., Hristovski, K., & Westerhoff, P. Functionalized nanoparticle interactions with polymeric membranes. *J. Hazard. Mater.*, doi:10.1016/j.jhazmat.2011.11.051 (2011).